A Satellite-linked Tag for the Long-term Monitoring of Diving Behavior in Large Whales

Daniel M. Palacios (daniel.palacios@oregonstate.edu)
Oregon State University https://orcid.org/0000-0001-7069-7913
Ladd M. Irvine
Oregon State University
Barbara A. Lagerquist
Oregon State University
James A. Fahlbusch
Stanford University Hopkins Marine Station
John Calambokidis
Cascadia Research Collective
Stanley M. Tomkiewicz
Telonics, Inc
Bruce R. Mate
Oregon State University

Research Article

Keywords: Argos satellite telemetry, bio-logging, smart tags, accelerometry, adaptive algorithm, event detection, diving behavior, lunge-feeding, rorqual whales, cetaceans

Posted Date: August 8th, 2022

DOI: https://doi.org/10.21203/rs.3.rs-834159/v2

A satellite-linked tag for the long-term monitoring of diving behavior in large whales

Daniel M. Palacios[1,2,†,*], Ladd M. Irvine[1,2,†], Barbara A. Lagerquist[1,2], James A. Fahlbusch[3,4], John Calambokidis[4], Stanley M. Tomkiewicz[5] and Bruce R. Mate[1,2]

[1]Marine Mammal Institute, Oregon State University, Newport, Oregon, USA

[2]Department of Fisheries, Wildlife, and Conservation Sciences, Oregon State University, Newport, Oregon, USA

[3]Department of Biology, Hopkins Marine Station, Stanford University, Pacific Grove, California, USA

[4]Cascadia Research Collective, Olympia, Washington, USA

[5]Telonics, Inc., Mesa, Arizona, 85204, USA

[†]These two authors contributed equally

*Corresponding author:

Daniel M. Palacios

daniel.palacios@oregonstate.edu

Abstract

Despite spending most time underwater, the technology in use to track whales over large geographic ranges via satellite has been largely limited to locational data, with most applications focusing on characterizing their horizontal movements. We describe the development of the RDW tag, a new Argos-based satellite telemetry device that incorporates sensors for monitoring the movements and dive behavior of large whales over several months without requiring recovery. Based on an implantable design, the tag features a saltwater conductivity switch, a tri-axial accelerometer, and an optional pressure transducer, along with onboard software for data processing and detection of behavioral events or activities of interest for transmission. We configured the software to detect dives and create per-dive summaries describing behavioral events associated with feeding activities in rorqual whales. We conducted a validation by proxy of the dive summary and event detection algorithms using field data from a medium-duration archival tag. We also conducted a simulation exercise to examine how the expected data recovery would vary under different dive behavior scenarios and compared those results to empirical values from field deployments of the RDW tag on blue (*Balaenoptera musculus*) and humpback (*Megaptera novaeangliae*) whales. The dive summary algorithm accurately reported dive depth and duration, while the accuracy of the lunge-feeding event detection algorithm was dependent on the precision of the accelerometer data that was used, with a predicted accuracy of 0.74 for correctly classifying feeding dives from 1/64-G precision data and 0.95 from 1-mG precision data. Simulated data recovery was lower with sparser transmission schedules, shorter mean dive durations, and lower rates of successfully received transmissions. Empirical data recovery was lower than expected from the simulation, suggesting the effect of additional factors like data gaps. By measuring key aspects of the per-dive behavior of large whales over multi-

month timescales of movement, the RDW tags provide the ability to monitor previously unobservable behaviors across entire geographic ranges, extending the applications of satellite telemetry devices to new areas of whale physiology, behavior, ecology, and conservation.

Keywords

Argos satellite telemetry, data recovery, bio-logging, smart tags, accelerometry, adaptive algorithm, event detection, diving behavior, foraging, lunge-feeding, ecological scales, rorqual whales, cetaceans

Background

The field of wildlife tracking and bio-logging using electronic devices has experienced explosive growth in the last two decades thanks to important technological advances and decreasing costs, which have made it a widely accessible approach for the study of movement, both in terrestrial and aquatic animals (1,2). Despite the dawn of this "golden age of animal tracking," large whales remain among the most difficult species to study using these technologies. Whales are large, highly streamlined animals that cannot be captured for tag attachment. Additionally, deploying and recovering electronic devices at sea on animals that have the capability to move great distances in short periods of time involves complicated and expensive logistics (3). Furthermore, as with other air-breathing aquatic animals that spend most of their time underwater, data transmission to earth-orbiting satellite platforms is limited to the brief periods that a whale is at the surface and a receiving satellite is simultaneously passing overhead. While these challenges have been partially overcome at fine scales by high-resolution (but short-duration) archival tags (e.g. (4–6)), the constraints associated with the transmission of large amounts of data over

65 extended times together with the limited functionality of longer-duration tags has led to a dearth
66 of behavioral data at large spatio-temporal scales. This situation has restricted the scope of
67 questions that have been addressed regarding whale distribution, movement, behavior, and
68 ecology.

69 The primary technology for tracking the long-distance movements of large whales, in use since
70 1997, has been a "consolidated" tag design (7) linked to the Argos satellite system. The
71 electronics and retention elements of consolidated tags are typically incorporated into a single
72 tag housing that is implanted on the whale's dorsal surface, from which only the antenna and a
73 salt-water switch are external to minimize hydrodynamic drag (3,8,9). These non-recoverable
74 tags can stay attached for long periods of time (typically several months) before they fall off. In
75 addition to locational data, some consolidated tag models have included capabilities for reporting
76 surfacing intervals and summarized dive behavior data in the form of time spent in discrete depth
77 or temperature intervals (i.e., "histogram data") or as per-dive metrics such as dive duration and
78 maximum dive depth (10–14). While such summaries have provided useful information on
79 overall diving behavior and time budgets, these data cannot be used to make inferences about
80 actual prey encounters or prey captures, and so their value in terms of understanding feeding
81 behavior is limited.

82 Most of what we know about large whale diving behavior comes from short- and medium-
83 duration archival tags, which permit collection of continuous, sensor-rich data streams. For
84 example, from these bio-loggers we have learned that prey capture events in several whale
85 species are often associated with rapid changes in motion that can be identified by their
86 stereotypical signatures in accelerometer data (15–18). This information has been used to
87 examine topics like the kinematics of feeding behavior (6,19,20), feeding strategies in relation to

88 the local prey field (21–25), or behavioral responses to anthropogenic activities (26–29).
89 However, the typical deployment period of these devices is limited to < 24 h (if attached with
90 suction cups) or to a few days or weeks (if attached with subdermal anchors), and recovery of the
91 tags is required to download the complete data record (4,26,29–32).

92 At broader scales, whale foraging behavior has only been inferred indirectly from tracking data,
93 either from the characteristics of horizontal movement (e.g., from concentrated locations (33)) or
94 from summarized data (e.g., per-dive or histogram data (10,11)). However, the relationship
95 between inferred and direct measurements of whale feeding behavior across spatial and temporal
96 scales remains unverified (34) and may vary with the scale of observation (i.e., the "grain size";
97 (35,36)). As movement behavior is driven by resource tracking and food acquisition through a
98 hierarchy of processes that operate at multiple spatio-temporal scales (37), obtaining this
99 information is essential to quantify the variability of resource dynamics and foraging strategies,
100 to test predictions on emergent behavior, and to improve our overall understanding of how
101 whales perceive and respond to their environment (2,38). Now more than ever, this information
102 can be critical to guide biodiversity conservation in the face of rapid global change (1,2,38).

103 Here we present a new satellite telemetry device for tracking the movements and dive behavior
104 of large whales over several months without tag recovery. The tag, manufactured by Telonics,
105 Inc. (Mesa, Arizona, USA), collects dive duration from a salt-water switch, inertial motion from
106 a tri-axial accelerometer, and dive depth from a pressure transducer. The tag uses a
107 microprocessor-based approach (39) featuring data processing software for (a) detecting
108 behavioral events from accelerometer data using an adaptive algorithm to account for individual
109 variation in behavior, and (b) summarizing and compressing dive data streams for transmission
110 through the Argos system. While satellite-linked tag platforms featuring accelerometers and

associated software have been recently developed for detecting, abstracting, and transmitting behavioral measures of activity in other marine top predators (40–42), this is the first time that accelerometers with event detection software were used on a satellite-transmitting tag for large whales.

Methods

Tag development

Development of the tag proceeded incrementally between 2015 and 2017, during which time we tested a variety of tag and software configurations in collaboration with Telonics. The initial model (RDW-640) used the salt-water switch to distinguish between dives and surfacings, and these data were compressed and relayed via Argos. This model also included a tri-axial accelerometer, but the software for processing this data stream was not yet developed, so the sensor was not active. A subsequent model (RDW-665) added a pressure sensor, increased battery capacity, and implemented a behavioral event detection algorithm to analyze the accelerometer data stream in real time. The updated model generated a data summary for every dive, consisting of dive duration, maximum dive depth, and number of behavioral events detected. Software onboard the tag's microprocessor packaged these summaries into messages for transmission through Argos, completing the development of the device. As the RDW-665 model included all components and configurations that were used by the RDW-640 model, from this point forward we refer to all tag versions as the "RDW tag" unless specifically noted.

Tag components and design

131 The RDW tag follows the same design of other consolidated tags for large whales in use since
132 1997 (3), which consists of a main body, an antenna and external sensor endcap at the distal end,
133 a penetrating tip at the proximal end, and an anchoring system (Figure 1). The main body
134 consists of a stainless-steel cylinder 18.5 cm in length × 1.9 cm in diameter that houses a
135 motherboard, a certified Argos transmitter (401.650 MHz ± 30 kHz operational frequency), a
136 thermistor for internal tag temperature monitoring, a tri-axial accelerometer, and a lithium
137 battery pack (two DL2/3A Duracell® 1550 mAh 3 V cells in parallel). An external flexible whip
138 antenna (15.8-cm long) and a stalked salt-water switch (2.2-cm long), both constructed of single-
139 strand nitinol (1.27 mm in diameter), are connected to the transmitter and mounted on a
140 polycarbonate endcap (2.6 cm in external length) that seal the distal end of the cylinder with two
141 rubber O-rings. The endcap is held in place by four stainless-steel set screws drilled through the
142 stainless-steel cylinder. The port for the pressure sensor of the RDW-665 model is also mounted
143 on the endcap (Figure 1).

144 The endcap has two perpendicular stops (1.5 cm long × 0.9 cm wide × 0.6 cm thick) extending
145 laterally to prevent tags from embedding too deeply on deployment or from migrating inward
146 after deployment. The penetrating tip is attached to the main body by a threaded screw (1.17 cm
147 long × 0.64 cm in diameter) and fixed with a set screw to prevent unthreading after deployment.
148 It consists of a polyoxymethylene (Delrin®) nose cone into which a ferrule shaft with four
149 double-edged blades is pressed and secured with a transverse roll-pin to prevent unintentional
150 removal. The anchoring system consists of two rows of ten outwardly curved metal strips (each
151 strip was 3.2 cm long × 0.6 cm wide) mounted on the main body at the nose cone (proximal) end
152 (Figure 1). Total tag weight is approximately 300 g.

153 The tag's cylinder is partially coated with a long-dispersant polymer matrix (Resomer® or
154 Eudragit®) in which a broad-spectrum antibiotic (gentamicin sulfate) is mixed to allow for a
155 continual release of antibiotic into the tag site for an extended time to reduce the chances of
156 infection (Figure 1). Like other consolidated tags, the RDW tag was designed to be almost
157 completely implantable (except for the perpendicular stops, antenna, and salt-water switch), and
158 is ultimately shed from the whale due to hydrodynamic drag and/or the natural migration out of
159 the tissue as a foreign body response (3). The expected functional life of the RDW tags is 188 d
160 when transmitting 24 h per day with a 45-s repetition rate, and 95% of time spent underwater
161 (43). The ethics of the use of consolidated implantable tags on large whales are briefly discussed
162 in the *Ethics approval* section, below.

163 *Tag sensors*

164 Argos transmissions are only attempted when the tag is above the water's surface to save battery
165 power (39). The status of the salt-water switch (wet/dry) is used to record dive start and end
166 times to calculate dive duration. The onboard pressure transducer allows collection of dive depth
167 data with an accuracy of ±2 m down to 200 m and then to ±1% of deeper depths. A tri-axial
168 accelerometer is also included, and records data at 8-bit precision (1/64 G), with an accuracy of
169 ±0.003 G and a dynamic range of -2 to 2 G. The sampling rate of tag sensors is user-
170 programmable and for our trials it was set to 1 Hz (1 s) for the salt-water switch, 0.2 Hz (5 s) for
171 the pressure transducer, and 4 Hz (0.25 s) for the accelerometer. All versions of the RDW tag
172 used in this study were tested in a water-pressure chamber to depths of 500 m with no failures.

173 *Tag software*

174 *(a) Dive summary algorithm:*

Dive behavior is continuously recorded and summarized for "selected dives," defined as dives meeting user-specified criteria for depth and duration, to generate "dive summaries". For the tag deployments presented here, selected dives were identified as dives > 2 min in duration and > 10 m in depth. Summary parameters including the start date, time, and duration of each selected dive were recorded, along with the maximum depth of the dive. Other possible dive depth-related metrics can be reported by the tag, such as a summarized profile of individual dives based on a subset of inflection points or the percentage of time spent in user-defined depth bins (44), but we did not record them in this study.

(b) Event detection algorithm:

The RDW tag can optionally be programmed for behavior event detection within selected dives using the accelerometer to detect rapid changes in motion, such as those often associated with lunge-feeding, or as a more general measure of activity based on variability of the accelerometer data, with the results included in the dive summary. Accelerometer sensor data are processed by the tag's microprocessor using an adaptive event detection algorithm. Threshold parameters for the event detection algorithm are continually updated from the sensor data stream and informed future iterations of the algorithm, allowing it to adapt over time. This adaptability can account for differences in tag placement on the whale's body, which can affect the magnitude and potential offsets of a sensor's signal owing to site-specific differences in acceleration and mechanical processes (17,45,46). The event detection algorithm was specifically developed to detect lunge-feeding behavior in rorqual whales (family *Balaenopteridae*), which produces strong stereotypical signatures in acceleration data (47,48) that can be used as a measure of feeding effort.

197 For selected dives, events are inferred from the change in the acceleration vector ("jerk"), which
198 for high-resolution archival tags is calculated as the norm of the difference in consecutive
199 acceleration readings (17). However, for this application, the jerk calculation is integrated over
200 one full second (four measurements) by taking the magnitude of the vector difference in the
201 current accelerometer readings from those one second previous. This variation is used to
202 standardize each measurement to 1 s and to reduce the effect of spurious readings. Additionally,
203 accelerometer readings from the first 5 s and final 5 s of each selected dive are excluded to
204 eliminate artifacts from fluke stroking associated with the start or end of a dive (19), as well as
205 from ocean surface wave drag (20).

206 The development of the event detection algorithm went through two iterations:

207 Version 1: A study by Simon et al. (19) showed that rorqual feeding lunges produce distinct
208 peaks in jerk, so the initial event detection algorithm identified jerk values that exceeded the
209 mean jerk by a threshold of 3.5 standard deviations (sd), with a 30 s blanking time (17) between
210 identified events to account for prey handling. If the threshold was exceeded multiple times
211 during the blanking time, only the first instance was recorded. Software in the tag's
212 microprocessor allowed mean and sd of jerk values to be continually updated following each
213 selected dive, making them the mean and sd of jerk for all selected dives up to that point. By
214 updating criteria to identify lunge-feeding events, the algorithm was able to adapt over time and
215 converge on threshold values that better accounted for individual differences in accelerometer
216 readings.

217 Version 2: A subsequent study by Allen et al. (16) indicated that rorqual feeding lunges were
218 best characterized by a jerk value above a specified threshold (jerk maximum) followed by a

value below a lower threshold (jerk minimum), so we updated the event detection algorithm to identify instances when the jerk value exceeded a threshold of 1.5 sd above the mean, followed by a value less than one half of the mean occurring within 30 s after the jerk peak. Jerk values had to exceed the upper threshold for 2 s to qualify as a lunge-feeding event, to account for transitory crossings possibly generated by error. Lunge-feeding events for each selected dive were then counted after applying a 35 s blanking time, which retained the first event if multiple ones were detected. As with version 1, the threshold mean and sd jerk values were updated following each selected dive. Thresholds and blanking times were chosen based on those from Allen et al. (16), but modified to be more conservative due to the lack of additional information provided by a hydrophone in the high-resoultion archival tags used in Allen et al. and the lower sampling rate of RDW tags (4 Hz versus 50-500 Hz). Further description of the lunge detection methodology is presented in Irvine et al. (24).

(c) Data transmission via Argos:

The RDW tag makes use of a highly compressed data transmission protocol to increase throughput of summarized dive data via Argos. Dive summaries are collected into "dive summary messages," consisting of a variable number of consecutive (typically four to ten) selected dives, depending on the number of reported summary parameters and other data compression factors such as the similarity of data values being reported. The tag maintains a buffer that held up to ten dive summary messages in the tag's microprocessor random-access memory. When enough dive summaries are recorded to create a new dive summary message, it is added to the buffer. If there are already ten messages in the buffer, the oldest message is discarded to make space for the new message.

241 Tag transmissions can contain either one dive summary message (randomly selected from the
242 buffer) or a utility message consisting of the tag's current internal temperature and voltage for
243 diagnostic purposes. The update to version 2 of the event detection algorithm also added the
244 current jerk mean and sd values into utility messages to monitor trends in those criteria over
245 time.

246 **Validation approach**

247 In principle, field validation of data collected by the RDW tag would involve a quantitative
248 comparison of the dive summaries obtained through Argos with equivalent summaries generated
249 from data recorded onboard the tag after a deployment. However, consolidated tags are not
250 designed for recovery (3,7), so this was not an option. Instead, in addition to verifying sensor
251 functionality in the laboratory, we implemented a validation by proxy of our event-detection
252 algorithm by running the tag software on a continuous data record obtained by an archival tag
253 under field conditions. Additionally, we evaluated the impact of transmission regimes on data
254 recovery via Argos using simulations compared to empirical data obtained from field
255 deployments of the RDW tag.

256 *Sensor functionality*

257 During development, we tested prototype tags in the laboratory to evaluate sensor functionality
258 and ability to report dive summaries through the Argos system. We replicated dives of varying
259 depths, duration, and complexity by closing the salt-water switch and placing the tags in a
260 pressurized chamber to replicate water depth. Enough dives were replicated to fill multiple dive
261 summary messages, which were then transmitted during an Argos satellite pass and used to
262 confirm agreement between the maximum dive depths and durations of replicated dives and the

corresponding tag-summarized values. Additionally, diagnostic software in the tag allowed direct download of a short-duration segment of the continuous accelerometer record, which we used to confirm the sensor's ability to record rapid changes in orientation and acceleration resulting from a person manipulating the tag to simulate abrupt motion changes.

Dive summary and event detection algorithms

We implemented a proxy validation of the tag's dive summary and event detection algorithms. For this purpose, we used a continuous data record from a Wildlife Computers TDR10-F medium-duration archival tag (hereafter "TDR10 archival data") deployed on a blue whale (*Balaenoptera musculus*) for 17.8 d while it was foraging off southern California in summer 2017 (26,31). We examined the performance of the RDW tag dive summary and event detection algorithms by running the TDR10 archival data record through the RDW tag's algorithms and comparing this output to the corresponding dive summaries calculated from the TDR10 archival data using standard analytical workflows for dive data. Analyses were implemented in the R software for statistical computing, v. 4.0.2 (49). We note that, while the high resolution and precision of archival data are commonly used to investigate cetacean behavior, they are not guaranteed to fully represent the true behavior of a tagged whale. Thus, "known" events in the proxy validation analysis will refer to events known from the TDR10 archival data, rather than the true behavior of the whale.

As the TDR10 archival tag continuously recorded pressure (depth) and tri-axial accelerometer data at 32 Hz, we decimated the sensor data to 4 Hz to match the sampling rate of the RDW tag. Additionally, the TDR10 archival accelerometer data were recorded with a native precision of 1 mG, so we subsequently reduced it to 1/64 G to match the precision of the RDW tag

observations. We identified "TDR10 dives" as those > 10 m depth using the *find_dives()* function from the R package *tagtools* **Error! Hyperlink reference not valid.**(17,50). We then calculated the maximum depth and duration for each dive, as well as their start and end times using custom R scripts. Feeding lunges were identified manually using stereotypical kinematic signatures from the 32-Hz accelerometer data (i.e., the animal's depth, pitch, roll, and speed, (51)).

We used the RDW dive summary and event detection algorithms to generate dive summaries from the TDR10 archival data (hereafter "RDW dives") as they would be received through Argos during an *in-situ* deployment (i.e., dive start date-time, maximum dive depth, dive duration, and number of lunge-feeding events) based on the decimated 4-Hz pressure and 1/64-G accelerometer data. To validate the RDW dive summary algorithm, we matched known dive summaries from the TDR10 dives to corresponding RDW dives using the dive start date-times and used linear regression to quantify the correspondence between maximum dive depth and dive duration values. For the number of lunge-feeding events per dive, we used polychoric correlation to assess the relationship between the number of RDW-detected lunge-feeding events and the number of known feeding lunges identified in the TDR10 archival data summary. This analysis provided an approximation of a Pearson's correlation coefficient for two ordinal variables and was conducted using the R package *polycor* v. 0.7-10 (52).

The ordinal nature of the number of lunge-feeding events per dive limited the utility of typical classification analyses like confusion matrices. Instead, we grouped known dives from the TDR10 archival data for each ordinal level of feeding lunges per dive, and calculated a false negative rate as the number of false negatives in the RDW-detected lunge-feeding events divided by the number of dives in the TDR10 archival data summary for that level. A similar procedure

was conducted to calculate the false positive rate. These values represent the mean number of lunge-feeding events missed per dive and the mean number of incorrectly identified lunges per dive, respectively, for each ordinal level.

As indicated above, the precision of the accelerometer sensor of the RDW tags was limited to 1/64 G, while the TDR10 accelerometer data were natively recorded at 1 mG. This allowed us to repeat the proxy validation process at the higher precision to determine if sensor precision influenced the accuracy of the RDW event detection algorithm, offering the opportunity to improve future versions of the tag.

Synthetic metrics of feeding behavior

Ecological studies often require data to be considered at different grain sizes to investigate emergent patterns at different domains of scale (53–55). The RDW tag was developed to monitor large whale feeding behavior across ecologically relevant spatio-temporal scales (i.e., 10s to 1000s of km and days to months), such that further synthesis of event data into coarser-grained metrics of feeding behavior may offer insights at broader scales (35,54,55). We evaluated the ability of RDW data to describe patterns of feeding at the per-dive level (i.e., feeding versus non-feeding dives) and at the per-feeding-bout level (i.e., sequences of feeding dives) relative to the TDR10 archival data.

The classification of RDW-derived feeding dives was validated by comparison to known feeding dives identified from the TDR10 archival data using a confusion matrix calculated with the function *confusionMatrix()* in R package *caret* v. 6.0-86 (56). For this classification, we report the true positive detection rate as the number of correctly classified feeding dives divided by all known feeding dives, the false positive detection rate as the number of incorrectly classified

feeding dives divided by all known non-feeding dives, and the accuracy as the sum of correctly classified feeding and non-feeding dives divided by the total number of dives.

To assess temporal trends in feeding intensity through feeding bouts obtained from the RDW and TDR10 dive summaries, we graphically examined the probability density distribution of the period of time between feeding dives to identify a behavioral change point criterion where the right tail of the distribution stabilized at a low value. Feeding bouts were identified as sequences of dives where feeding dives were separated by a period no longer than the criterion. A period longer than the criterion was interpreted as the whale changing its behavior, or possibly leaving a feeding patch. We tested the RDW-derived probability density distribution for consistency with the distribution of values from TDR10 data using Bhattacharyya's similarity coefficient (57,58), where values < 0.05 and > 0.95 indicate that the distributions are significantly different, or similar, respectively, and intermediate values indicate the probability of overlap between the two distributions (57). The number of RDW-derived bouts was then compared to the number of known TDR10-derived bouts. As described above for the dive summary and event detection algorithms, the synthetic metrics described in this section were generated at the 1/64-G precision of the RDW accelerometer sensor as well as at the 1-mG precision of the TDR10 sensor.

Assessment of data recovery via Argos

Recovery of RDW dive summary data via Argos during field deployments is dependent on the coincident occurrence of the whale at the surface, with the tag scheduled to transmit, while a satellite is overhead to receive the transmission. If a dive summary message is replaced by a new message in the transmission buffer without having been received by a satellite, its data are lost. Thus, data recovery (i.e., the number of summarized dives received) will depend on the number of messages received by a satellite over a given time period. Whales making short-duration dives

will generate more dive summary messages per day than whales making long-duration dives, filling the transmission buffer more quickly and potentially replacing messages before they are received by a satellite. Further, longer time periods spent at the surface will allow more messages to be transmitted compared to shorter surface periods, increasing the likelihood of a satellite being overhead when a message is transmitted.

To characterize the expected data recovery during an RDW tag deployment we conducted simulation experiments where time series of dives for a hypothetical whale were generated under a range of behavioral and tag programming regimes, to test their effect on data recovery. The results of these simulations were then compared to empirical values collected from field deployments conducted on blue and humpback (*Megaptera noveaeangliae*) whales off California during summer of 2017. A dive time series was composed of sequences of dives followed by post-dive intervals (PDI) during which a whale is near the surface for a cycle of respirations before the next dive. We generated two representative time series of dives (n = 4,000), matched in time to real satellite pass intervals, by sequentially drawing a dive duration from log-normal distribution, then calculating a corresponding PDI based on predictions from a linear model fit to dive duration and PDI values gleaned from Dolphin (59) and Acevedo-Gutiérrez et al. (60) (PDI = 0.07944 + 0.29333 × duration). A "short-dive" time series simulated a whale making short-duration dives (mean = 3 min, sd = 1.5 min), while a "long-dive" time series consisted of longer-duration dives (mean = 9 min, sd = 1.3 min). These values were intended to broadly reflect the dive behavior of humpback (59) and blue whales (60,61), respectively, although the species designation is ultimately unimportant, as we expect similar results from other species with similar dive behavior. The 4,000-dive length of the time series was chosen so the time series

would last multiple weeks, allowing for a range of daily satellite pass durations to be incorporated.

For each simulated dive time series, different tag programming regimes were implemented to determine their effect on data recovery. Sequential groups of seven dives from a time series were identified to replicate RDW tag dive summary messages and added to (and later removed from) a simulated transmission buffer holding ten messages. Daily simulated transmissions occurred either during six, 1-h periods ("6-h schedule") scheduled to coincide with the most likely time a satellite would be overhead, or during alternating hours of the day ("12-h schedule") to replicate the range of compromises that Argos users often have to make between continuously transmitting and conserving battery power by reducing the number of transmissions. Satellite pass predictions were obtained with the satellite pass prediction tool available to users of the Argos system via their website (62) for the area off Newport, OR, USA (45°N, 124°W).

During each PDI when simulated transmissions were scheduled to occur, a dive summary message was randomly selected with replacement from the transmit buffer every 30, 60, or 120 s (transmit interval) and assumed to have been transmitted. The different transmit intervals are meant to reflect individual and interspecific differences in a whale's respiration cycle while at the surface, which controls when tags can transmit. Data from a transmitted dive summary message were considered "received" if the transmission time coincided with a predicted satellite pass and it was retained after accounting for an empirically determined message corruption rate of 44% (detailed in the next section). We ran simulations for both short- and long-dive time series with all combinations of tag programming conditions and calculated the proportion of all dive summaries received (after excluding duplicates) compared to the true number of dives in the simulated time series. Hourly plots of the number of received dives were also made to examine

temporal trends in data recovery that might be related to patterns of satellite coverage and/or transmit schedule.

Field deployments

To provide an empirical comparison to proxy validation results and simulated predictions, we obtained the event-detection threshold values and characterized data recovery and message corruption for 28 RDW tags deployed on blue (n = 14) and humpback whales (n = 14) off southern and central California during July-August 2017 (63,64). Seven humpback whale tags were RDW-660 (which only reported dive start time and duration), while the other seven tags were RDW-665 (which recorded dive start time, duration, maximum dive depth, and number of lunge-feeding events). All blue whale tags were RDW-665. To conserve battery power and maximize operational tag life, RDW-660 tags were programmed to transmit when at the surface for five 1-h periods each day, while RDW-665 tags were programmed to transmit for six1-h periods. Both RDW tag models were programmed with a 10-s transmit repetition rate when at the surface. These transmission periods were selected based on satellite pass predictions for the time and location of tag deployment, available to users of the Argos system via their website (62).

For each tag deployment, we used the received data to extract the event-detection threshold values (mean and sd jerk) from utility messages and summarized them based on their minimum, maximum and last values reported. We also identified and removed corrupted messages of all types using the Cyclic Redundancy Check (CRC) code, and determined the proportion of corrupted messages relative to the total number of received messages. We then calculated the number of unique daily dive summary messages received and plotted the number of received

dives by hour for comparison to simulated results. We also calculated the percent of both the simulated and empirical time series data that was summarized by received transmissions as the sum of all received dive durations and PDIs divided by the total duration of the time series. During field deployments, dive end times were calculated as the sum of the dive start time and duration, while PDI was calculated as the difference between a dive start time and the end time of the previous dive. As the PDI value for the last dive in a dive summary message cannot be calculated, the complete dive time series cannot be recovered. For this reason, we removed the last PDI value from each received dive summary message in our simulation study to better match the empirical data when calculating the percent of the tracking period summarized.

Results

Proxy validation of dive summary data

1/64-G precision data

The RDW dive summary algorithm identified 2,462 selected dives and 1,302 lunge-feeding events (range = 0-11 per dive; Figure A1 in Additional file) when implemented on TDR10 archival data at the reduced precision of the accelerometer sensor of the RDW tags used in field deployments (1/64 G). Of these, 753 dives contained at least one feeding lunge, and were consequently classified as feeding dives. A total of 6,317 feeding lunges (range = 0-12 per dive) were manually identified in 1,345 feeding dives when generating known dive summaries from the TDR10 archival data. There was a near-perfect correlation between the two sets of dive summaries for both maximum dive depth and duration (Spearman's rank correlation, $\rho = 1$; Figures A2 and A3 in Additional file).

441 The threshold values (mean and sd of jerk) of the RDW event detection algorithm stabilized
442 quickly and had no variation after about 80 dives over the initial 13 h of the 17.8-d tracking
443 period (mean jerk = 2/64 G/s, sd jerk = 4/64 G/s; Figure A4 in Additional file). The number of
444 detected RDW lunge-feeding events per dive was positively correlated with the number of
445 feeding lunges detected in the TDR10 archival data (polychoric correlation $r = 0.63$; Figure 2).
446 The false negative rate by lunges per dive ranged from 0.56 to 5.6 (excluding a single 12-lunge
447 dive that the event-detection algorithm missed by 1 lunge), while the false positive rate ranged
448 from 0 to 0.02 (Table A2 in Additional file).

449 The accuracy of the RDW event detection algorithm when classifying feeding/non-feeding dives
450 at 1/64-G precision was 0.74 when compared to known feeding dives from the TDR10 archival
451 data (Table 1). The true-positive detection rate was 0.55, indicating many feeding dives were not
452 correctly identified by the RDW event detection algorithm. However, the false-positive detection
453 rate was 0.018, indicating that, when a feeding dive was identified, it was almost always
454 correctly classified.

455 The probability density distribution of time between feeding dives showed a high degree of
456 overlap between RDW and TDR10 data (Bhattacharyya's similarity coefficient = 0.82). Most
457 times between feeding dives occurred at ≤ 60 min (Figure A5 in Additional file), indicating 60
458 min as a good criterion to identify the end of a feeding bout. Using this criterion, the RDW data
459 generated 70 feeding bouts, 21 of which were single-dive bouts. Since our goal for identifying
460 feeding bouts was to illustrate how coarse-grained metrics of feeding activity could be generated
461 from RDW tag data, single-dive bouts were removed, resulting in a total of 49 feeding bouts,
462 compared to 20 known feeding bouts recorded by TDR10 data (none of which were single-dive
463 bouts).

1-mG precision data

Implementing the RDW event detection algorithm at the native (1-mG) resolution of the TDR10 archive data resulted in the detection of 4,452 lunge-feeding events (range = 0-10 per dive; Figure A1 in Additional file) and 1,372 feeding dives, compared to 6,317 known lunge-feeding events and 1,345 feeding dives in the TDR10 archive. The threshold values (mean and sd of jerk) of the RDW event detection algorithm converged on initial ranges of ± 5 mG/s for both parameters after about 110 dives over the initial 19 h of the 17.8-d TDR10 tag deployment, and eventually stabilized to consistent values after approximately one week (mean jerk = 49.9 mG/s, sd jerk = 67.5 mG/s; Figure A4 in Additional file). The number of RDW lunge-feeding events per dive detected from 1-mG data was closely positively correlated with the number of known feeding lunges from the TDR10 archive data (polychoric correlation $r = 0.88$; Figure 2). The mean false negative rate by lunges per dive ranged from 0.29 to 1.83 (excluding two single-dive ordinal levels with one and two false negatives), while the false positive rate ranged from 0 to 0.22 (Table A2 in Additional file).

The accuracy of the RDW event detection algorithm when classifying a feeding dive at the native (1-mG) resolution of the TDR10 archive data was 0.95 when compared to known feeding dives identified from the TDR10 archive data (Table 1). The true-positive detection rate was 0.96, while the false-positive detection rate was 0.067, indicating that the vast majority of feeding dives were correctly classified by 1-mG RDW dives.

The probability density distribution of time between feeding dives showed a high degree of overlap between RDW and TDR10 dives (Bhattacharyya's similarity coefficient = 0.83). Most times between feeding dives occurred at ≤ 60 min (Figure A6 in Additional file), indicating a

good criterion to identify the end of a feeding bout. Using this threshold, the RDW data generated 31 feeding bouts, 11 of which were single-dive bouts. When single-dive bouts were removed, RDW data reported 20 feeding bouts, which was the same as recorded by TDR10 data.

Data recovery via Argos

As expected, simulated data recovery increased with decreasing transmit intervals (i.e., more received dive summary messages), while longer mean dive duration and PDI increased the proportion of simulated dive summaries that were recovered (Table 2). The 6-h transmit schedule resulted in the recovery of 80.8-97.5% of long-dive summaries across all transmit intervals compared to 53.2-74.6% for short-dive summaries. This represents a relative increase in data recovery of 20.6% and 40.2% respectively for a quadrupling of the dive summary messages transmitted between the shortest and longest transmit intervals. More than 84% of the simulated dive summaries were recovered across both short- and long-dives when the 12-h schedule was used (Table 2), with a relative increase in data recovery of 14.3% for short-dive summaries and only 1.2% for long-dive summaries across the range of transmit intervals. For the short-dive time series, gaps were present in the daily pattern of recovered dives when using the 6-h transmit schedule and were centered on gaps in transmit times, related to satellite coverage (Figure 3, Additional file Figure A6). In these instances, most dives were recovered for the period 3-4 h before a scheduled transmission hour. No data gaps were present in the daily pattern of recovered dives for the long-dive time series, although for longer transmit intervals (60 s, 120 s), fewer dives were recovered during hours near the start of long gaps in satellite coverage (Table 2, Figure 3, Additional file Figure A6).

Field deployments

508 Event-detection threshold values received from RDW tag utility messages were generally higher
509 than those calculated by the proxy validation using the TDR10 archival data, with mean jerk
510 thresholds for blue whales ranging from 5/64 to 16/64 G/s (sd jerk range: 9/64-19/64 G/s) and
511 from 9/64 to 19/64 G/s (sd jerk range: 6/64-18/64 G/s) for humpback whales (Table A1 in
512 Additional file). The median percentage of corrupted messages for blue whales was 44% (range:
513 28-58%) for blue whales and 18% (range: 10-32%) for humpback whales (Table A3 in
514 Additional file). Fewer dive summaries were recovered from RDW tags deployed on blue and
515 humpback whales than would be expected from the simulation of data recovery rates. A mean of
516 8.8 (sd = 5.2) unique dive summary messages were received per day from tags attached to blue
517 whales, summarizing a mean of 45.8% (sd = 15.0%) of the tracking duration (Table 2, Figure 4).
518 Fewer unique daily dive summary messages were received from humpback whales tagged with
519 RDW-660 tags (mean = 5.6, sd = 3.3; transmit schedule: five 1-h periods) compared to those
520 tagged with RDW-665 tags (mean = 11.1, sd = 4.6; transmit schedule: six1-h periods), which
521 resulted in a smaller percentage of the tracking period being summarized (mean = 33.9% versus
522 71.1%, sd = 15.0% versus 8.3%, respectively). However, by reporting one less parameter
523 (maximum dive depth), RDW-660 tags were able to transmit over 40% more dives per dive
524 summary message compared to RDW-665 tags (mean = 10.1 versus 7.0 dives per transmission,
525 respectively; Figure 4C).

526 # Discussion

527 ### Proxy validation of dive summary data

528 The RDW dive summary and event detection algorithms were able to capture with varying
529 success the observed dive and feeding behavior of a blue whale tracked for 17.8 d with a TDR10

530 tag, whose archival record was used for validation. Maximum dive depth and duration were
531 reported with high accuracy, while accuracy was low for the 1/64-G precision accelerometer data
532 when reporting the number of lunge-feeding events made during a dive. However, the higher
533 accuracy and very low false-positive detection rate when classifying dives as feeding or non-
534 feeding, as well as the similarity of feeding bout metrics derived from RDW and TDR10 data,
535 indicate that these data are useful for coarser-grained characterizations of feeding behavior.
536 Further, the performance of the event detection algorithm was significantly improved in all
537 aspects by increasing the precision of accelerometer readings from 1/64 G to 1 mG.

538 The small mean jerk values calculated from the TDR10 archival data (~ 2/64 G/s; Figure A4 in
539 Additional file), and used as thresholds to trigger an event detection, meant that the minimum
540 jerk criteria (less than half the mean jerk) could not be resolved well at 1/64-G resolution. The
541 added precision of the 1-mG data better resolved these small values, allowing for a greater
542 number of possible values that met the minimum jerk criteria, resulting in improved detection
543 performance. All new versions of the RDW tag now support 1-mG precision accelerometer data.
544 (Parenthetically, the RDW event detection algorithm at the 1/64-G precision may have
545 performed better during field deployments than our validation results indicated, as empirical
546 mean and sd jerk threshold values were larger than those reported for the TDR10 data, allowing
547 a greater ability to resolve values below the minimum jerk criteria).

548 Probability density curves for time between feeding dives were generally similar in shape for
549 both 1/64- and 1-mG data, although when the behavioral change point criterion was applied,
550 1/64-G data produced more bouts, including numerous single-dive bouts. This result was likely
551 due to the high number of false-negative feeding dives identified by the RDW event detection
552 algorithm at 1/64 G, which divided feeding bouts observed in the TDR10 archival data into

multiple shorter bouts. An implementation of this feeding bout analysis is not currently feasible for field deployments of RDW tags, as limitations of satellite coverage, whale surfacing behavior, and other factors affecting tag transmission can result in often incomplete time series of dive summaries (see results from the data recovery rate simulation; Figure 3). However, planned improvements to the Argos satellite constellation, as well as other recent developments to improve reception of satellite transmissions (65,66) raise the possibility of better data recovery in the future, leading to an improved ability to characterize feeding behavior at varying spatial and temporal scales.

Data recovery via Argos

The simulation exercise suggested that very high data recovery rates should be possible, and, although the empirical results did not perform as well, these results, and the relative differences in data recovery, provided insights for how users can plan deployments and maximize the amount of data collected. The rate of transmissions received by the satellite (reception rate) is the primary constraint on data recovery, so increasing the daily transmit hours will boost data recovery, as demonstrated by the difference in percent of the time series summarized between 6-h and 12-h daily transmission schedules (Table 2). However, the gain in received transmissions from increased transmit hours will come with a trade-off of higher battery consumption rate, and further depend on species-specific variation in behaviors like surfacing rates, which might limit opportunities for a tag to transmit, as well as potential differences in message corruption rate as suggested by our empirical estimates (67).

The time period summarized by each transmission is an additional constraint on the data recovery rate. Assuming reception rates are equivalent, a greater proportion of the tracking

575 period will be summarized from animals making long-duration dives compared to shorter dives
576 (as observed with the long-dive time series). Each dive summary message will report a longer
577 portion of the tracking period, and fewer messages need to be received to summarize the entire
578 track. If a target species makes short-duration dives, the time period recorded by a dive summary
579 message can be expanded to boost data recovery by selecting only longer-duration dives to
580 summarize, provided it fits with the research goals. Similarly, the time period summarized by a
581 transmission is dependent on the number of dives it reports, with more dives representing a
582 longer summary time period. By reporting one less parameter, the RDW-660 tags reported a
583 mean of ten dives per transmission, compared to seven by RDW-665 tags. In this case, the gain
584 in data recovery was likely offset by the reduction of transmission hours from 6 to 5 but it offers
585 an additional way to increase data recovery depending on the needs of the study.

586 Argos satellite coverage is not ubiquitous, and the effect of coverage gaps was observed in the
587 temporal pattern of reduced hourly data recovery (Figure 3). During longer gaps in satellite
588 coverage, dive summary messages can pass through the transmission buffer without a satellite
589 ever having been overhead, especially if new messages are generated quickly, as was the case for
590 the short-dive time series. Shorter satellite-coverage-related data gaps can be expected for
591 animals making longer-duration dives (as shown by the long-dive time series), as each dive
592 summary message will report a longer portion of the tracking period, bridging more of the gap in
593 satellite coverage.

594 Our empirical assessment of data recovery from field deployments of the RDW tag was lower
595 than the expectation from our simulation exercise. This is not entirely surprising, as satellite
596 tracking data, especially in the marine realm, are oftentimes affected by poorly understood or
597 undetermined extrinsic factors that result in data gaps and that reduce the amount of data

reported (see next section). The transmission schedule for these tags was set as a compromise between data recovery and battery longevity, and future deployments will use different protocols to meet the needs of each specific project.

Limitations

Recovery of data from instrumented animals is a significant hurdle for research, especially when conducted on large whales, which can move > 100 km per day and do not return to a central place where a tag can reliably be recovered (3,68). For RDW tags, data recovery is limited by the coincident occurrence of the tagged whale surfacing while an Argos satellite is overhead to receive a transmission. As shown by our simulations, the duration of recorded dives can also affect data recovery, as longer dives will summarize a greater portion of the tracking period with each transmission. Collectively, this means that dive summary time series from RDW tags are rarely complete, and the number of dives reported from each tag can vary widely depending on individual behavior and transmission schedule. Further, even if recovery of the entire summarized time series is achieved, it must be understood that dives not meeting selected dive criteria are not recorded by the RDW tag. Extrinsic factors like bad weather or biofouling can also affect data recovery by limiting or corrupting satellite transmissions. The biases associated with these dive summaries are related to the degree of irregularity and the scale of the behavior being studied (69,70), but a more adequate characterization will require dedicated research. For these reasons, RDW tags should be considered to provide a relative index of dive behavior, rather than a continuous and complete record.

We assumed that the received dives were a random sample of selected dives that occurred during the tracking period. However, the process of grouping consecutive dives for transmission may

introduce bias through serial correlation, while the whales' surfacing patterns and tag duty cycling may further contribute to a lack of independence in ways that remain to be characterized. Thus, more research is needed to assess how dive summaries are received, if animal behavior might affect these trends, and how the relevant scales of behavior being studied might be affected. For this reason, *in-situ* validation of detected events by means of using concurrently attached bio-loggers on whales carrying RDW tags remains a high priority.

Conclusions

The correspondence between RDW and TDR10 dive summaries and their derived feeding bouts in the proxy validation exercise demonstrated that RDW tags can link local-scale behavior to broader, regional, or ecosystem-scale processes by monitoring per-dive behavior over multi-month timescales of movement. A previous study using medium-duration tags (24) showed that the number of feeding lunges made per dive is related to the duration of feeding bouts in both blue and fin whales, suggesting that longer-term behavioral monitoring can more fully describe the drivers of residence time over the course of the feeding season. Additionally, these behaviorally mediated processes like sex-based habitat partitioning or diel changes in depth related to prey distribution can lead to variable or differential exposure to anthropogenic impacts (24,26,71), making this information highly useful to management and conservation organizations.

Conceptually, the flexible sensor configuration and adaptive software capabilities of RDW tags makes them generalizable for a variety of applications with cetaceans, which may extend to studies of species that use other foraging tactics like raptorial feeding or ram-filtration (72). Known behavioral cues associated with non-feeding behaviors could also be incorporated into

642 the event detection algorithm, for example to investigate patterns and trends in male singing
643 (73,74) or agonistic interactions (75). The tags could also be used to monitor changes in body
644 condition over time based on trends in buoyancy, as implemented through hydrodynamic glide
645 models (76–78). Such information could further inform studies of the effects of anthropogenic
646 disturbance on individuals and how related changes in fitness might scale up to the larger
647 population (e.g., (79,80)).

648 Advances in microprocessor technology continue to reduce component size, operating voltage,
649 and current consumption, while at the same time increasing the available on-board memory and
650 processing speed. Future improvements to the software (e.g., refinement of event detection
651 algorithms) and advances in hardware (e.g., addition of other environmental sensors and
652 increasing sensor precision) will further expand RDW tag applications for ecology, management,
653 and conservation. The RDW tag joins a new generation of devices with the technological
654 capacity to collect and, in some cases, process large volumes of data onboard (26,41,81). These
655 advances pave the way for the routine generation of key metrics of dive behavior for marine
656 wildlife onboard non-recoverable smart tags across large spatial and temporal scales, while the
657 ability to dynamically update event detection parameters (e.g., to account for differences in tag
658 placement or behavioral trends) offers opportunities for improved long-term behavioral and
659 physiological monitoring.

660 # Declarations

661 ## Ethics approval

662 The activities reported in this study involving deployment of RDW tags on large whales were
663 carried out under the authorization of U.S. National Marine Fisheries Service Marine Mammal

664 Protection Act and Endangered Species Act scientific research permit No. 14856 and Oregon
665 State University Institutional Animal Care and Use Committee Permit Nos. 4495 and 4884,
666 issued to Bruce R Mate. The activities involving deployment of the TDR10-F archival tag on
667 large whales were carried out under U.S. National Marine Fisheries Service permit No. 16111-02
668 issued to John Calambokidis.

669 Implantable electronic tags for large whales are increasingly used as tools for collecting
670 information on physiology, behavior, and ecology, and for enhancing conservation and
671 management policies for their populations (7). We recognize, however, that while not well-
672 understood, tags and tagging procedures may have detrimental effects on the subject animals
673 during any of the phases of the research, including approach, deployment, operation, detachment,
674 and post-detachment (7). We approach whales and deploy tags in a manner that mitigates
675 disturbance, stress, and harm to the subject animals. To the extent possible, we also conduct
676 follow-up field observations and/or obtain photographs of tagged animals from a network of
677 collaborators and citizen scientists to increase re-sightings for documentation of wound healing,
678 survival, body condition, and reproductive success in the short, medium, and long term. While
679 we have not documented significant effects from our current technology, our tag development
680 philosophy is aligned with the principles of reducing tag size and improving tag deployment
681 equipment (82,83), while also striving to expand device capabilities and produce richer data
682 streams from the same form factor. However, we also recognize the potential for additional
683 impacts relating to the discomfort experienced by a whale swimming with an implanted tag for
684 extended periods of time. There is evidence that discomfort from tags on wildlife may vary
685 widely by taxa and lifestyle (84,85). In large whales, one study suggested that placement of
686 implanted tags high on the body near the dorsal midline and anterior to the dorsal fin will

687 mitigate tissue damage and trauma (86). However, a significant information gap remains in our
688 understanding of the level of discomfort associated with implanted intra-muscular tags on
689 whales.

690 **Consent for publication**

691 Not applicable.

692 **Availability of data and materials**

693 The datasets supporting the conclusions of this article, including the 4-Hz, 1/64-G TDR10 data,
694 will be deposited in a Movebank Repository (https://www.datarepository.movebank.org) upon
695 acceptance.

696 **Competing interests**

697 ST is Director of Telonics, Inc., which developed the RDW tags for commercial use. As the
698 manufacturer, Telonics may benefit from the publication of this manuscript.

699 **Funding**

700 Funding for tagging blue and humpback whales off California in 2017 was provided by the U.S.
701 Department of the Navy, Commander, Pacific Fleet, and Commander, Naval Sea Systems
702 Command, under the Navy's Marine Species Monitoring Program via contract with HDR, Inc.
703 (Contract No. N62470-15-D-8006) and through a Cooperative Ecosystem Studies Unit
704 agreement (Cooperative Agreement No. N62473-17-2-0001). Both projects were administered
705 by Naval Facilities Engineering Command (NAVFAC) Southwest. We thank Jessica Bredvik
706 and Reagan Pablo at NAVFAC for serving as the Technical Representative and the Agreement

707 Administrator of these awards, respectively. We also thank Kristen Ampela at HDR, Inc. for
708 project management and contractual support. Activities conducted by Cascadia Research
709 Collective reported in this paper were funded in part by the U.S. Office of Naval Research and
710 the U.S. National Marine Fisheries Service.

711 **Author's contributions**

712 BM conceived of and secured the funding for the RDW tag. ST led the design and development
713 of the RDW devices for Telonics, Inc. LI contributed to the development of event detection
714 algorithms. LI and BL conducted the testing of sensor functionality in the lab and contributed to
715 the RDW field data collection. DP and LI conceived the conceptual approach of the manuscript.
716 LI and DP analyzed the data. JF and JC collected the TDR10 data, analyzed the TDR10 record,
717 and contributed to RDW validation. DP and LI drafted the manuscript with contributions from
718 BL, JF, ST, and BM. All authors read and approved the final manuscript.

719 **Acknowledgements**

720 We thank Telonics engineers Jeff Tenney and Chris Lusko for their invaluable support in the
721 technical development and validation of the RDW tags. We gratefully acknowledge the support
722 in the field provided by the crew of the R/V *Pacific Storm* in California. We also thank the
723 people who assisted with tagging operations, including Ken Serven, Martha Winsor, Craig
724 Hayslip, Tomas Follett, Kris Bauer, Steve Lewis, Will Sheehy, Kyle Milliken, and Colin Gillin.
725 At the Oregon State University Marine Mammal Institute, we acknowledge Tomas Follett for
726 database management and Kathy Minta, Mark Wilke, and Minda Stiles for logistical and
727 administrative support. Finally, we thank Beto Alvarez for drafting Figure 1.

The Argos Data Collection and Location System was used for this project (62). The system is operated by Collecte Localisation Satellites. Argos is an international program that relies on instruments provided by the French Space Agency flown on polar-orbiting satellites operated by the U.S. National Oceanic and Atmospheric Administration, the European Organisation for the Exploitation of Meteorological Satellites, and the Indian Space Research Organization.

References

1. Kays R, Crofoot MC, Jetz W, Wikelski M. Terrestrial animal tracking as an eye on life and planet. Science. 2015;348(6240).

2. Hussey NE, Kessel ST, Aarestrup K, Cooke SJ, Cowley PD, Fisk AT, et al. Aquatic animal telemetry: A panoramic window into the underwater world. Science. 2015;348(6240).

3. Mate B, Mesecar R, Lagerquist B. The evolution of satellite-monitored radio tags for large whales: One laboratory's experience. Deep Sea Research Part II: Topical Studies in Oceanography. 2007;54(3):224–47.

4. Johnson MP, Tyack PL. A digital acoustic recording tag for measuring the response of wild marine mammals to sound. IEEE Journal of Oceanic Engineering. 2003;28(1):3–12.

5. Burgess WC. The Acousonde: A miniature autonomous wideband recorder. The Journal of the Acoustical Society of America. 2009;125(4):2588–2588.

6. Goldbogen JA, Cade DE, Boersma AT, Calambokidis J, Kahane-Rapport SR, Segre PS, et al. Using digital tags with integrated video and inertial sensors to study moving morphology and associated function in large aquatic vertebrates. The Anatomical Record. 2017;300(11):1935–41.

7. Andrews RD, Baird RW, Calambokidis J, Goertz CEC, Gulland FMD, Heide-Jørgensen MP, et al. Best practice guidelines for cetacean tagging. Journal of Cetacean Research and Management. 2019;20:27–66.

8. Heide-Jørgensen MP, Kleivane L, ØIen N, Laidre KL, Jensen MV. A new technique for deploying satellite transmitters on baleen whales: Tracking a blue whale (Balaenoptera musculus) in the North Atlantic. Marine Mammal Science. 2001;17(4):949–54.

9. Zerbini AN, Andriolo A, Heide-Jørgensen MP, Pizzorno JL, Maia YG, VanBlaricom GR, et al. Satellite-monitored movements of humpback whales Megaptera novaeangliae in the Southwest Atlantic Ocean. Marine Ecology Progress Series. 2006;313:295–304.

10. Citta JJ, Quakenbush LT, Okkonen SR, Druckenmiller ML, Maslowski W, Clement-Kinney J, et al. Ecological characteristics of core-use areas used by Bering–Chukchi–Beaufort (BCB) bowhead whales, 2006–2012. Progress in Oceanography. 2015;136:201–22.

11. Weinstein BG, Irvine L, Friedlaender AS. Capturing foraging and resting behavior using nested multivariate Markov models in an air-breathing marine vertebrate. Movement Ecology. 2018;6(1):16.

12. Derville S, Torres LG, Zerbini AN, Oremus M, Garrigue C. Horizontal and vertical movements of humpback whales inform the use of critical pelagic habitats in the western South Pacific. Scientific Reports. 2020;10(1):1–13.

13. Lagerquist BA, Mate BR, Ortega-Ortiz JG, Winsor M, Urbán-Ramirez J. Migratory movements and surfacing rates of humpback whales (Megaptera novaeangliae) satellite tagged at Socorro Island, Mexico. Marine Mammal Science. 2008;24(4):815–30.

14. Chambault P, Fossette S, Heide-Jørgensen MP, Jouannet D, Vély M. Predicting seasonal movements and distribution of the sperm whale using machine learning algorithms. Ecology and Evolution. 2021;11(3):1432–45.

15. Miller PJO, Johnson MP, Tyack PL. Sperm whale behaviour indicates the use of echolocation click buzzes 'creaks' in prey capture. Proceedings of the Royal Society of London Series B: Biological Sciences. 2004;271(1554):2239–47.

16. Allen AN, Goldbogen JA, Friedlaender AS, Calambokidis J. Development of an automated method of detecting stereotyped feeding events in multisensor data from tagged rorqual whales. Ecology and Evolution. 2016;6(20):7522–35.

17. Sweeney DA, DeRuiter SL, McNamara-Oh YJ, Marques TA, Arranz P, Calambokidis J. Automated peak detection method for behavioral event identification: detecting Balaenoptera musculus and Grampus griseus feeding attempts. Animal Biotelemetry. 2019;7(1):7.

18. Goldbogen JA, Cade DE, Calambokidis J, Friedlaender AS, Potvin J, Segre PS, et al. How baleen whales feed: The biomechanics of engulfment and filtration. Annual Review of Marine Science. 2017;9(1):367–86.

19. Simon M, Johnson M, Madsen PT. Keeping momentum with a mouthful of water: behavior and kinematics of humpback whale lunge feeding. Journal of Experimental Biology. 2012;215(21):3786–98.

20. Owen K, Dunlop RA, Monty JP, Chung D, Noad MJ, Donnelly D, et al. Detecting surface-feeding behavior by rorqual whales in accelerometer data. Marine Mammal Science. 2016;32(1):327–48.

21. Goldbogen JA, Hazen EL, Friedlaender AS, Calambokidis J, DeRuiter SL, Stimpert AK, et al. Prey density and distribution drive the three-dimensional foraging strategies of the largest filter feeder. Functional Ecology. 2015;29(7):951–61.

22. Hazen EL, Friedlaender AS, Goldbogen JA. Blue whales (Balaenoptera musculus) optimize foraging efficiency by balancing oxygen use and energy gain as a function of prey density. Science Advances. 2015;1(9):e1500469.

23. Cade DE, Seakamela SM, Findlay KP, Fukunaga J, Kahane-Rapport SR, Warren JD, et al. Predator-scale spatial analysis of intra-patch prey distribution reveals the energetic drivers of rorqual whale super-group formation. Functional Ecology. 2021;35(4):894–908.

24. Irvine LM, Palacios DM, Lagerquist BA, Mate BR. Scales of blue and fin whale feeding behavior off California, USA, with implications for prey patchiness. Frontiers in Ecology and Evolution. 2019;7.

25. Irvine L, Palacios DM, Urbán J, Mate B. Sperm whale dive behavior characteristics derived from intermediate-duration archival tag data. Ecology and Evolution. 2017;7(19):7822–37.

26. Calambokidis J, Fahlbusch JA, Szesciorka AR, Southall BL, Cade DE, Friedlaender AS, et al. Differential vulnerability to ship strikes between day and night for blue, fin, and humpback whales based on dive and movement data from medium duration archival tags. Frontiers in Marine Science. 2019;6.

27. DeRuiter SL, Langrock R, Skirbutas T, Goldbogen JA, Calambokidis J, Friedlaender AS, et al. A multivariate mixed hidden Markov model for blue whale behaviour and responses to sound exposure. Annals of Applied Statistics. 2017;11(1):362–92.

28. Goldbogen JA, Southall BL, DeRuiter SL, Calambokidis J, Friedlaender AS, Hazen EL, et al. Blue whales respond to simulated mid-frequency military sonar. Proceedings of the Royal Society B: Biological Sciences. 2013;280(1765):20130657.

29. Owen K, Jenner CS, Jenner MNM, Andrews RD. A week in the life of a pygmy blue whale: migratory dive depth overlaps with large vessel drafts. Animal Biotelemetry. 2016;4(1):17.

30. Mate BR, Irvine LM, Palacios DM. The development of an intermediate-duration tag to characterize the diving behavior of large whales. Ecology and Evolution. 2017;7(2):585–95.

31. Szesciorka AR, Calambokidis J, Harvey JT. Testing tag attachments to increase the attachment duration of archival tags on baleen whales. Animal Biotelemetry. 2016;4(1):18.

32. Baumgartner MF, Hammar T, Robbins J. Development and assessment of a new dermal attachment for short-term tagging studies of baleen whales. Methods in Ecology and Evolution. 2015;6(3):289–97.

825 33. Bailey H, Mate BR, Palacios DM, Irvine L, Bograd SJ, Costa DP. Behavioural estimation of
826 blue whale movements in the Northeast Pacific from state-space model analysis of
827 satellite tracks. Endangered Species Research. 2009;10:93–106.

828 34. Palacios DM, Bailey H, Becker EA, Bograd SJ, DeAngelis ML, Forney KA, et al. Ecological
829 correlates of blue whale movement behavior and its predictability in the California Current
830 Ecosystem during the summer-fall feeding season. Movement Ecology. 2019;7(1):26.

831 35. Kotliar NB, Wiens JA. Multiple Scales of Patchiness and Patch Structure: A Hierarchical
832 Framework for the Study of Heterogeneity. Oikos. 1990;59(2):253–60.

833 36. Wheatley M, Johnson C. Factors limiting our understanding of ecological scale. Ecological
834 Complexity. 2009;6(2):150–9.

835 37. Johnson DH. The comparison of usage and availability measurements for evaluating
836 resource preference. Ecology. 1980;61(1):65–71.

837 38. Abrahms B, Aikens EO, Armstrong JB, Deacy WW, Kauffman MJ, Merkle JA. Emerging
838 perspectives on resource tracking and animal movement ecology. Trends in Ecology &
839 Evolution. 2020;36(4):308–20.

840 39. Tomkiewicz MSM. Development of intelligent PTTs with emphasis on sensor technology
841 applicable to wildlife research programs. [Internet]. Pages 97-104 in Parc national du
842 Mercantour, “Suivi par radiotélémétrie des vertébrés terrestres,” Actes du Colloque
843 International, Monaco, 12 - 13 décembre 1988.; 1989. Available from:
844 https://documentation.ensg.eu/index.php?lvl=notice_display&id=35287

845 40. Heerah K, Hindell M, Guinet C, Charrassin JB. From high-resolution to low-resolution dive
846 datasets: a new index to quantify the foraging effort of marine predators. Animal
847 Biotelemetry. 2015;3(1):42.

848 41. Skubel RA, Wilson K, Papastamatiou YP, Verkamp HJ, Sulikowski JA, Benetti D, et al. A
849 scalable, satellite-transmitted data product for monitoring high-activity events in mobile
850 aquatic animals. Animal Biotelemetry. 2020;8(1):34.

851 42. Pohlot BG, Ehrhardt N. An analysis of sailfish daily activity in the Eastern Pacific Ocean
852 using satellite tagging and recreational fisheries data. ICES Journal of Marine Science.
853 2018;75(2):871–9.

854 43. Argos transmitters for Cetaceans [Internet]. [cited 2022 May 31]. Available from:
855 https://www.telonics.com/products/argosMarine/cetacean.php

856 44. Fedak MA, Lovell P, Grant SM. Two Approaches to Compressing and Interpreting Time-
857 Depth Information as Collected by Time-Depth Recorders and Satellite-Linked Data
858 Recorders. Marine Mammal Science. 2001;17(1):94–110.

45. Martín López LM, Miller PJO, Aguilar de Soto N, Johnson M. Gait switches in deep-diving beaked whales: biomechanical strategies for long-duration dives. Journal of Experimental Biology. 2015;218(9):1325–38.

46. Wilson RP, Börger L, Holton MD, Scantlebury DM, Gómez-Laich A, Quintana F, et al. Estimates for energy expenditure in free-living animals using acceleration proxies: A reappraisal. Journal of Animal Ecology. 2020;89(1):161–72.

47. Calambokidis J, Schorr GS, Steiger GH, Francis J, Bakhtiari M, Marshall G, et al. Insights into the underwater diving, feeding, and calling behavior of blue whales from a suction-cup-attached video-imaging tag (Crittercam). Marine Technology Society; 2007.

48. Goldbogen JA, Calambokidis J, Croll DA, Harvey JT, Newton KM, Oleson EM, et al. Foraging behavior of humpback whales: kinematic and respiratory patterns suggest a high cost for a lunge. Journal of Experimental Biology. 2008;211(23):3712–9.

49. Core Team R. R: A language and environment for statistical computing. [Internet]. R Foundation for statistical computing. Vienna, Austria.; 2020. Available from: https://www.R-project.org/.

50. TagTools [Internet]. [cited 2022 May 31]. Available from: https://github.com/stacyderuiter/TagTools

51. Cade DE, Friedlaender AS, Calambokidis J, Goldbogen JA. Kinematic diversity in rorqual whale feeding mechanisms. Current Biology. 2016;26(19):2617–24.

52. Fox J. polycor: Polychoric and Polyserial Correlations [Internet]. R package version 0.7-10.; 2019. Available from: https://CRAN.R-project.org/package=polycor.

53. Levin SA. The Problem of Pattern and Scale in Ecology: The Robert H. MacArthur Award Lecture. Ecology. 1992;73(6):1943–67.

54. McGarigal K, Wan HY, Zeller KA, Timm BC, Cushman SA. Multi-scale habitat selection modeling: a review and outlook. Landscape Ecol. 2016;31(6):1161–75.

55. Wiens JA. Spatial Scaling in Ecology. Functional Ecology. 1989;3(4):385–97.

56. Kuhn M, Wing J, Weston S, Williams A, Keefer C, Englehardt A, et al. caret: Classification and Regression Training. [Internet]. R package version 6.0-84; 2019. Available from: https://CRAN.R-project.org/package=caret

57. Guillerme T, Cooper N. Effects of missing data on topological inference using a Total Evidence approach. Molecular Phylogenetics and Evolution. 2016;94:146–58.

58. Bhattacharyya A. On a measure of divergence between two statistical populations defined by their probability distributions. Bulletin of the Calcutta Mathematical Society. 1943;35:99–109.

59. Dolphin WF. Ventilation and dive patterns of humpback whales, Megaptera novaeangliae, on their Alaskan feeding grounds. Canadian Journal of Zoology. 1987;65(1):83–90.

60. Acevedo-Gutiérrez A, Croll DA, Tershy BR. High feeding costs limit dive time in the largest whales. Journal of Experimental Biology. 2002;205(12):1747–53.

61. Goldbogen JA, Cade DE, Calambokidis J, Czapanskiy MF, Fahlbusch J, Friedlaender AS, et al. Extreme bradycardia and tachycardia in the world's largest animal. Proceedings of the National Academy of Sciences. 2019;116(50):25329–32.

62. Argos [Internet]. [cited 2022 May 31]. Available from: https://www.argos-system.org

63. Mate BR, Palacios DM, Baker CS, Lagerquist BA, Irvine LM, Follett T, et al. Baleen Whale Tagging in Support of Marine Mammal Monitoring Across Multiple Navy Training Areas Covering the Years 2014, 2015, 2016, and 2017 [Internet]. 2018 p. 180. (Prepared for Commander, U.S. Pacific Fleet. Submitted to Naval Facilities Engineering Command Southwest under Contract No. N62470-15-8006-17F4016 issued to HDR, Inc., San Diego, California.). Available from: https://www.navymarinespeciesmonitoring.us/files/2415/5484/0267/Mate_et_al_2018_Baleen_Whale_Tagging_on_US_West_Coast.pdf

64. Mate BR, Palacios DM, Baker CS, Irvine LM, Lagerquist BA, Follett TM, et al. Humpback Whale Tagging in Support of Marine Mammal Monitoring Across Multiple Navy Training Areas in the Pacific Ocean [Internet]. 2018 p. 160. (Final Report for Feeding Areas off the US WestCoast in Summer-Fall 2017, Including Historical Data from Previous Tagging Efforts. Prepared forCommander, US Pacific Fleet and Commander, Naval Sea Systems Command. Submitted to NavalFacilities Engineering Command Southwest, San Diego, California, under Cooperative EcosystemStudies Unit, Department of the Navy Cooperative Agreement No. N62473-17-2-0001.). Available from: https://www.navymarinespeciesmonitoring.us/files/1915/5484/0269/Mate_et_al_2018_Humpback_Whale_Tagging_on_US_West_Coast_Summer-Fall_2017.pdf

65. Jeanniard-du-Dot T, Holland K, Schorr GS, Vo D. Motes enhance data recovery from satellite-relayed biologgers and can facilitate collaborative research into marine habitat utilization. Animal Biotelemetry. 2017;5(1):17.

66. Billie M, Dendiu R, Baker L, Brune S, Byrnes I, Round C. Microsats and moby dick: microsatellite support to whale science and conservation. In: Proceedings, 32nd Annual AIAA/USU Conference on Small Satellites. Paper number SSC18-V-07. 1-11.; 2018.

67. Quick NJ, Cioffi WR, Shearer J, Read AJ. Mind the gap—optimizing satellite tag settings for time series analysis of foraging dives in Cuvier's beaked whales (Ziphius cavirostris). Animal Biotelemetry. 2019;7(1):5.

68. Mate BR, Lagerquist BA, Calambokidis J. Movements of North Pacific blue whales during the feeding season off southern California and their southern fall migration. Marine Mammal Science. 1999;15(4):1246–57.

69. Mul E, Blanchet MA, Biuw M, Rikardsen A. Implications of tag positioning and performance on the analysis of cetacean movement. Animal Biotelemetry. 2019;7(1):11.

70. Breed GA, Costa DP, Goebel ME, Robinson PW. Electronic tracking tag programming is critical to data collection for behavioral time-series analysis. Ecosphere. 2011;2(1):art10.

71. Keen EM, Falcone EA, Andrews RD, Schorr GS. Diel Dive Behavior of Fin Whales (Balaenoptera physalus) in the Southern California Bight. Aquatic Mammals. 2019;45(2):233–43.

72. Heithaus MR, Dill LM, Kiszka JJ. Feeding strategies and tactics. In: Wursig B, Thewissen JGM, Kovacs KM, editors. Encyclopedia of Marine Mammals - 3rd Edition. Cambridge, MA, USA: Academic Press; 2018. p. 354–63.

73. Oestreich WK, Fahlbusch JA, Cade DE, Calambokidis J, Margolina T, Joseph J, et al. Animal-borne metrics enable acoustic detection of blue whale migration. Current Biology. 2020;30(23):4773-4779.e3.

74. Stimpert AK, DeRuiter SL, Falcone EA, Joseph J, Douglas AB, Moretti DJ, et al. Sound production and associated behavior of tagged fin whales (Balaenoptera physalus) in the Southern California Bight. Animal Biotelemetry. 2015;3(1):23.

75. Baker CS, Herman LM. Aggressive behavior between humpback whales (Megaptera novaeangliae) wintering in Hawaiian waters. Canadian Journal of Zoology. 1984;62(10):1922–37.

76. Aoki K, Isojunno S, Bellot C, Iwata T, Kershaw J, Akiyama Y, et al. Aerial photogrammetry and tag-derived tissue density reveal patterns of lipid-store body condition of humpback whales on their feeding grounds. Proceedings of the Royal Society B: Biological Sciences. 2021;288(1943):20202307.

77. Miller P, Narazaki T, Isojunno S, Aoki K, Smout S, Sato K. Body density and diving gas volume of the northern bottlenose whale (Hyperoodon ampullatus). Journal of Experimental Biology. 2016;219(16):2458–68.

78. Narazaki T, Isojunno S, Nowacek DP, Swift R, Friedlaender AS, Ramp C, et al. Body density of humpback whales (Megaptera novaengliae) in feeding aggregations estimated from hydrodynamic gliding performance. PLOS ONE. 2018;13(7):e0200287.

79. Pirotta E, Schwarz LK, Costa DP, Robinson PW, New L. Modeling the functional link between movement, feeding activity, and condition in a marine predator. Behavioral Ecology. 2019;30(2):434–45.

80. Pirotta E, Booth CG, Cade DE, Calambokidis J, Costa DP, Fahlbusch JA, et al. Context-dependent variability in the predicted daily energetic costs of disturbance for blue whales. Conservation Physiology. 2021;9(1):coaa137.

81. Cox SL, Orgeret F, Gesta M, Rodde C, Heizer I, Weimerskirch H, et al. Processing of acceleration and dive data on-board satellite relay tags to investigate diving and foraging behaviour in free-ranging marine predators. Methods in Ecology and Evolution. 2018;9(1):64–77.

82. Kay WP, Naumann DS, Bowen HJ, Withers SJ, Evans BJ, Wilson RP, et al. Minimizing the impact of biologging devices: Using computational fluid dynamics for optimizing tag design and positioning. Methods in Ecology and Evolution. 2019;10(8):1222–33.

83. Holton MD, Wilson RP, Teilmann J, Siebert U. Animal tag technology keeps coming of age: an engineering perspective. Philosophical Transactions of the Royal Society B: Biological Sciences. 2021;376(1831):20200229.

84. Wilson RP, Rose KA, Gunner R, Holton MD, Marks NJ, Bennett NC, et al. Animal lifestyle affects acceptable mass limits for attached tags. Proceedings of the Royal Society B: Biological Sciences. 2021;288(1961):20212005.

85. Wilson RP, McMahon CR. Measuring devices on wild animals: what constitutes acceptable practice? Frontiers in Ecology and the Environment. 2006;4(3):147–54.

86. Moore MJ, Zerbini AN. Dolphin blubber/axial muscle shear: implications for rigid transdermal intramuscular tracking tag trauma in whales. Journal of Experimental Biology. 2017;220(20):3717–23.

Additional files

additional_file.pdf

Title: Additional file: Additional tables and figures

Description: This file contains two tables and five figures providing supplementary information related to the proxy validation of the RDW tag dive summary and event detection algorithms. It also includes one table providing per-tag information on data corruption from transmission through Argos, and one figure with simulation of data recovery through Argos using a 12-h transmission schedule.

996 **Table 1**. Confusion matrix showing the classification of feeding and non-feeding dives by
997 version 2 of the RDW-665 event detection algorithm compared to dives summarized from
998 continuous Wildlife Computers TDR10-F archive data. True positive (TP) and false positive
999 (FP) detection rates are presented in the right margin.

1000

		TDR10 archive dives		
		Feeding	Non-feeding	
1/64-G RDW dives	Feeding	733	20	TP rate = 0.55
	Non-feeding	612	1,097	FP rate = 0.018
1-mG RDW dives	Feeding	1,297	75	TP rate = 0.96
	Non-feeding	48	1,042	FP rate = 0.067

1001

1002

1003 **Table 2**. Summary results for a simulation exercise investigating the effect of different dive

1004 behaviors and Argos transmission regimes on data recovery.

Daily transmission schedule	Transmit interval (s)	Mean (sd) unique daily received transmissions	% of time series summarized	Mean (sd) unique daily received transmissions	% of time series summarized
		Short-dive time series		Long-dive time series	
6 h	30	34.1 (8.4)	74.60%	16.9 (2.8)	97%
	60	28.5 (7.4)	62.80%	16.3 (2.9)	93.30%
	120	24.5(6.9)	53.20%	14.2 (2.9)	80.80%
12 h	30	44.5 (9.6)	96.10%	17.1 (2.3)	97%
	60	43.1 (9.6)	92.90%	17 (2.5)	96.30%
	120	38.3 (8.9)	84.10%	16.8 (2.6)	95.80%
Field Deployments		Humpback		Blue	
RDW-665 (6 h)		11.1 (4.6)	71.1% (18.3)	8.8 (5.2)	45.8% (15.0)
RDW-660 (5 h)		5.6 (3.3)	33.9% (15.0)		

1005

1006

1007

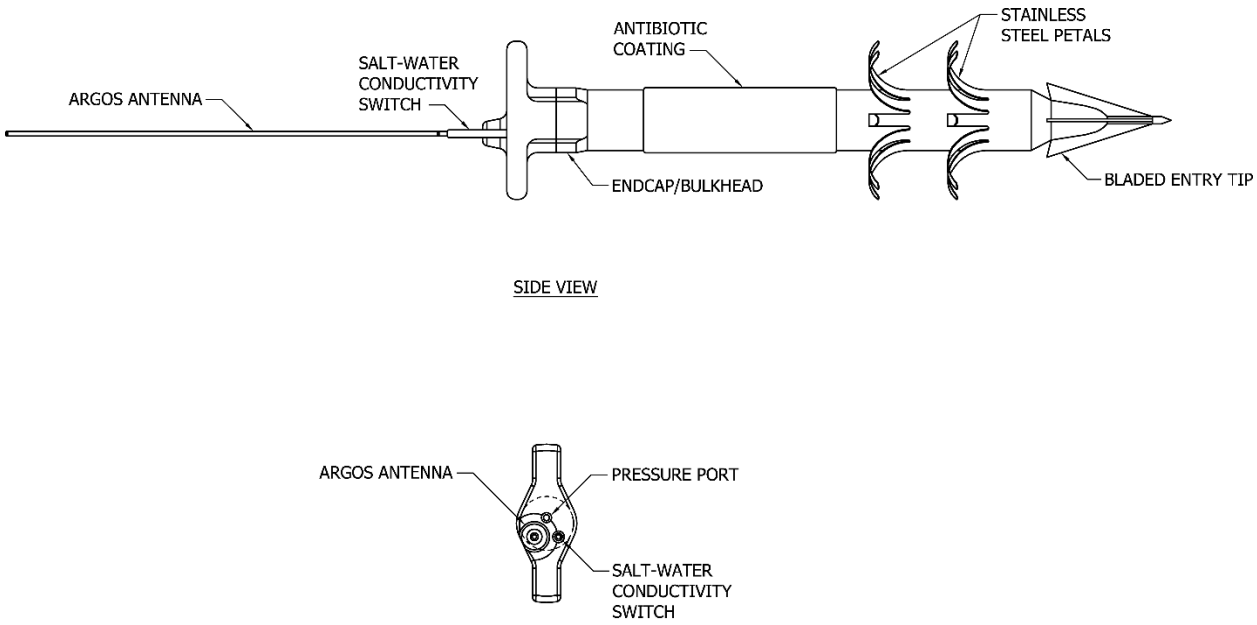

Figure 1. Schematic diagram of a fully assembled Telonics RDW-665 tag. Side view (top drawing) shows, from left to right, the distal endcap with the exposed Argos antenna and salt-water conductivity switch, the main body partially coated with antibiotic, and the penetrating tip and anchoring system with two rows of stainless-steel strips ("petals") in deployed position. Top view (bottom drawing) shows the placing of the salt-water switch and the pressure transducer on the endcap. Both views show the two stop tabs extending laterally from the endcap to prevent the tag from embedding too deeply into the whale.

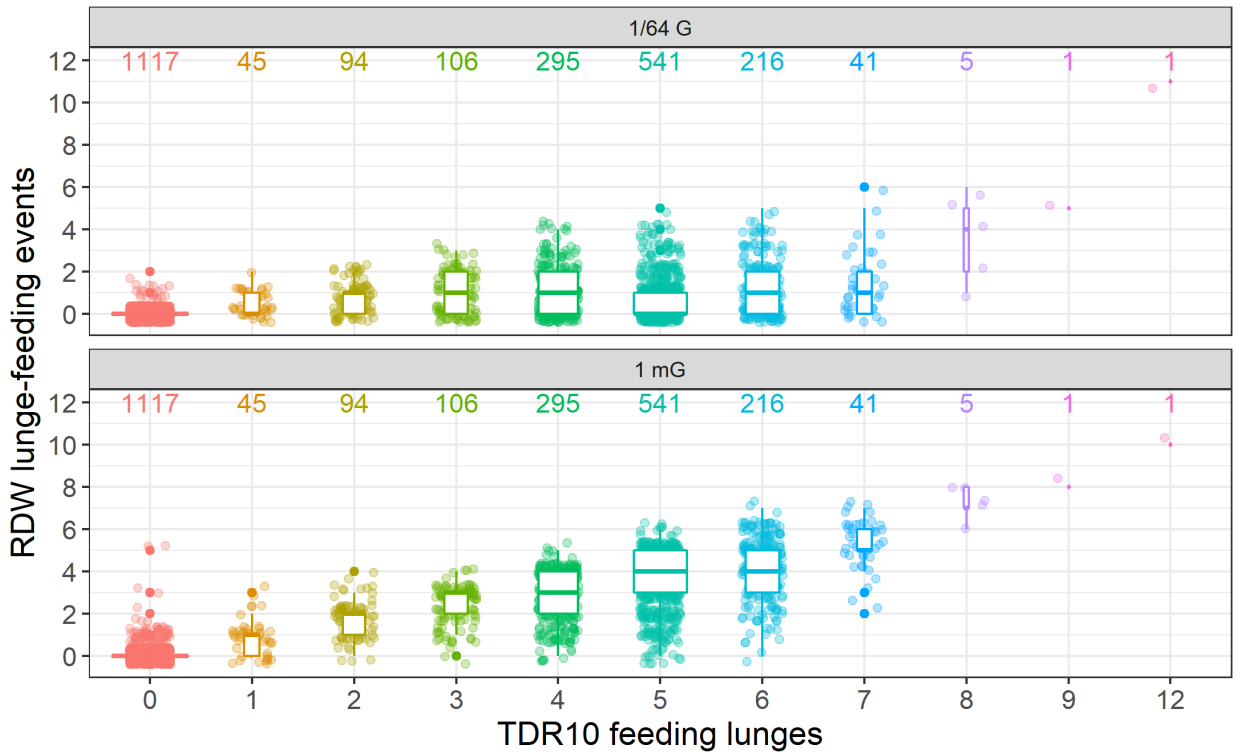

Figure 2. Boxplots of the results of the proxy validation of the RDW tag's event detection algorithm showing the number of detected lunge-feeding events per dive as a function of the known number of feeding lunges per dive determined from a 17.8-d TDR10 archival record of a blue whale. Top panel shows results for 1/64-G data while the bottom panel shows results for 1-mG data. Width of boxes is proportional to the sample size for that category and the numbers at the top of the plot represent the number of dives in that category. Data points are jittered on both axes for better visibility.

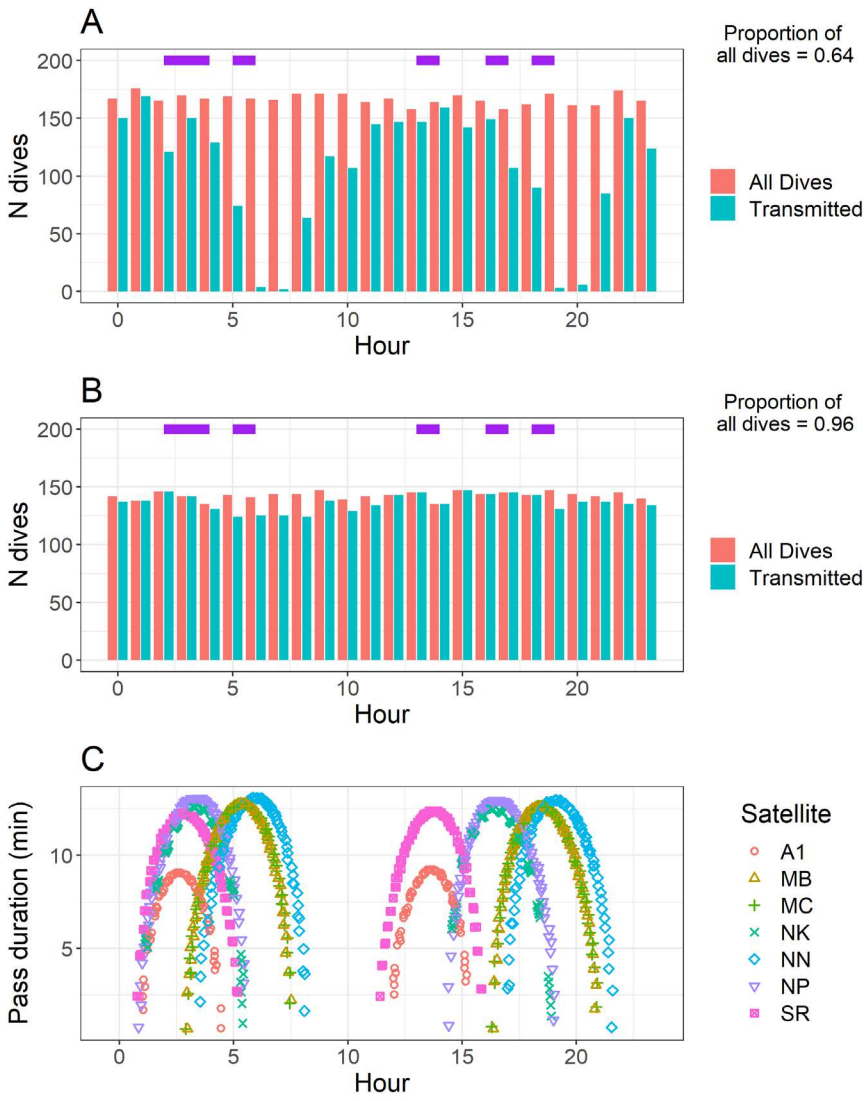

1030

1031 **Figure 3**. Simulation results to test the effect of RDW tag dive summary and transmission
1032 regimes on data recovery. Dives were simulated for an animal making relatively short-duration
1033 dives (e.g., humpback whales; A) and long-duration dives (e.g., blue whales; B). Dive summary
1034 messages were assumed to have been transmitted every 60 s during six 1-h periods (purple
1035 horizontal bars) scheduled to coincide with the greatest chance of a predicted satellite pass (C).
1036 Dive summaries were assumed to have been received if a satellite was predicted to be overhead
1037 when the message was transmitted.

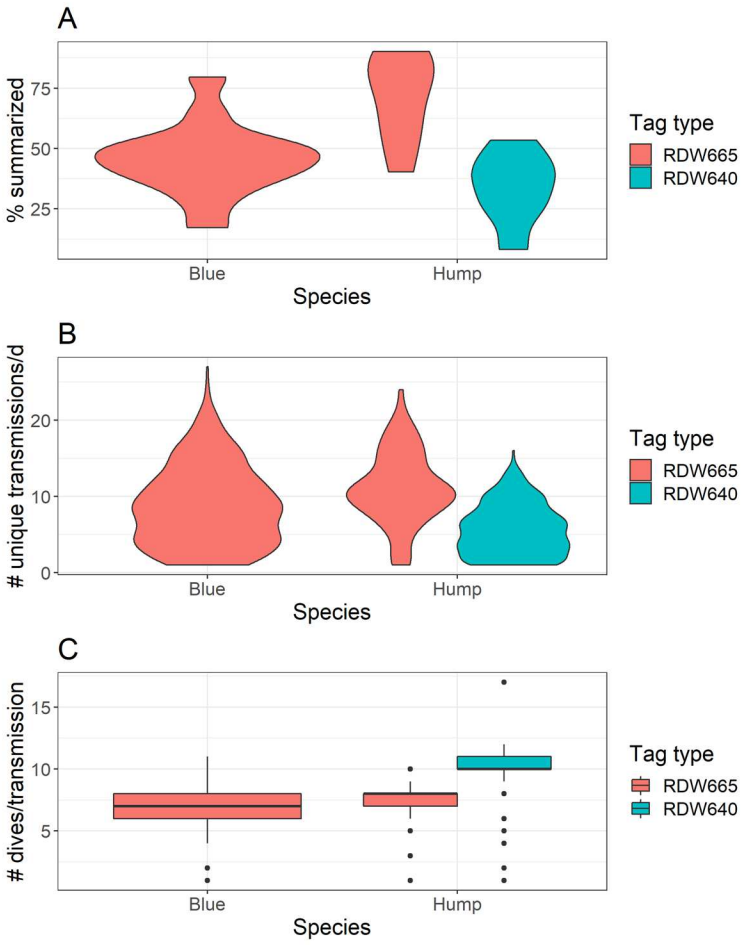

Figure 4. Percent of tracking period summarized (A), number of unique dive summary messages received per day (B), and number of received dive summaries per transmission (C) from RDW tags deployed on humpback and blue whales off California during summer 2017.

Supplementary Files

This is a list of supplementary files associated with this preprint. Click to download.

- additionalfile.pdf